

# Exploring Hidden Sectors with Two-Particle Angular Correlations at Future $e^+e^-$ Colliders

Emanuela Musumeci <sup>1</sup>, Adrián Irlés <sup>1,\*</sup>, Redamy Pérez-Ramos <sup>2,3</sup>, Imanol Corredoira <sup>4</sup>, Edward Sarkisyan-Grinbaum <sup>5,6</sup>, Vasiliki A. Mitsou <sup>1</sup> and Miguel Ángel Sanchis-Lozano <sup>1</sup>

<sup>1</sup> IFIC – Universitat de València and CSIC, 46980 Paterna, Spain; emanuela.musumeci@ific.uv.es (E.M.); adrian.irlés@ific.uv.es (A.I.); vasiliki.mitsou@ific.uv.es (V.A.M.); mas@ific.uv.es (M.A.S.L.)

<sup>2</sup> DRII-IPSA, 94200 Ivry-sur-Seine, France; redamy.perez-ramos@ipsa.fr

<sup>3</sup> Laboratoire de Physique Théorique et Hautes Energies (LPTHE), UMR 7589, Sorbonne Université et CNRS, 75252 Paris Cedex 05, France

<sup>4</sup> Instituto Galego de Física de Altas Enerxías (IGFAE), Universidade de Santiago de Compostela, 15782 Santiago de Compostela, Spain; imanol.corredoira.fernandez@cern.ch

<sup>5</sup> Experimental Physics Department, CERN, 1211 Geneva 23, Switzerland; edward.sarkisyan-grinbaum@cern.ch

<sup>6</sup> Department of Physics, The University of Texas at Arlington, Arlington, TX 76019, USA

\* Correspondence: adrian.irlés@ific.uv.es

**Abstract:** Future  $e^+e^-$  colliders are called to play a fundamental role in measuring Standard Model (SM) parameters with unprecedented precision and discovering physics beyond the SM (BSM). This study scrutinises two-particle angular correlation distributions involving final-state SM charged hadrons. Unexpected correlation structures in these distributions could be a hint for new physics perturbing the QCD partonic cascade and modifying azimuthal and (pseudo)rapidity correlation. Using PYTHIA8 and detector fast simulation tools we study unexpected structures arising in the two-particle angular correlation function, including selection cuts and detector effects. We have chosen the QCD-like Hidden Valley (HV) scenario as implemented in PYTHIA8, with relatively light  $v$ -quarks ( $\lesssim 100$  GeV), to illustrate the potential of this method.

**Keywords:**  $e^+e^-$  colliders; angular correlations; ridge feature; New Physics; Hidden Valley; Higgs factories

## 1. Introduction

Correlations play a fundamental role in the study of hadronic dynamics since the beginning of cosmic ray and accelerator physics [1,2]. Recently, the study of angular correlations have revealed a new phenomenon in heavy-ion collisions, later also found in smaller system (proton–proton, proton–nucleus) collisions [3–5]

In particular, long-range near-side (so-called) ridges show up in two-particle angular correlations, while different theoretical explanations have been put forward to understand this initially unexpected phenomenon [6–11]. Almost all of them require the existence of some unconventional state of matter at the primary interaction of the collision (like quark-gluon plasma), ultimately yielding collective effects among final-state SM particles. On the other hand, no clear ridge-like signal was found in the  $e^+e^-$  data analysed by ALEPH [12] and Belle [13] experiments, except for recent claims in [14] at the highest available energy and high multiplicity of the former.

Motivated by such unexpected correlation structures found in high-energy collisions, we look at possible anomalies (not only ridge effects) in both azimuthal and (pseudo) rapidity correlations to gain a useful insight into an unknown stage of matter on top of the QCD parton shower. We focus on two-particle angular correlations as a way of searching for BSM at future high-energy  $e^+e^-$  colliders, providing a much cleaner environment than hadron colliders in several theoretical and experimental respects. For instance, QCD effects on matter under extreme temperature and density conditions (e.g. leading to the Glass-Gluon Condensate [15]) cannot be reached in  $e^+e^-$  collisions due to the lack

of gluonic fields at the initial state and beam remnants. Let us also emphasize that the scope of the present study remains circumscribed to the search for new phenomena in leptonic collisions, and not in hadron colliders like the LHC.

The theoretical framework of New Physics (NP) used in this work is based on the so-called *Hidden Valley* (HV) scenario, which actually stands for a wide class of models with one or more hidden sectors beyond the SM. Thereby, new (valley) particles of mass  $\lesssim 100$  GeV arise, still surviving all discovery limits at present, contributing to the partonic cascade yielding final SM particles.

## 2. Two-particle angular correlations

The clean environment of  $e^+e^-$  collisions, in contrast to hadronic collisions, is especially suitable to define a reference frame whose  $z$ -axis lies along the direction of the back-to-back jets in most events. The thrust reference frame has been used throughout this work, so the rapidity  $y$  of a particle always refers to the thrust- or  $z$ -axis. The azimuthal angle  $\phi$  is defined, as usual, on the transverse plane to the thrust axis, event by event. Note that only rapidity and azimuthal differences of two final-state SM charged particles labelled as ‘1’ and ‘2’,  $\Delta y \equiv y_1 - y_2$ ,  $\Delta\phi \equiv \phi_1 - \phi_2$ , will be used in our study.

The two-particle correlation function is defined as

$$C^{(2)}(\Delta y, \Delta\phi) = \frac{S(\Delta y, \Delta\phi)}{B(\Delta y, \Delta\phi)}, \quad (1)$$

where  $S(\Delta y, \Delta\phi)$  stands for the density of particle pairs within the same event

$$S(\Delta y, \Delta\phi) = \frac{1}{N_{\text{pairs}}} \frac{d^2 N_{\text{same}}}{d\Delta y d\Delta\phi}, \quad (2)$$

while  $B(\Delta y, \Delta\phi)$  represents the density of mixed particle pairs from distinct events

$$B(\Delta y, \Delta\phi) = \frac{1}{N_{\text{mix}}} \frac{d^2 N_{\text{mix}}}{d\Delta y d\Delta\phi}. \quad (3)$$

The so-called azimuthal yield,  $Y(\Delta\phi)$ , is of particular interest, being defined by integration over a given  $\Delta y$  range as:

$$Y(\Delta\phi) = \frac{\int_{y_{\text{inf}} \leq |\Delta y| \leq y_{\text{sup}}} S(\Delta y, \Delta\phi) dy}{\int_{y_{\text{inf}} \leq |\Delta y| \leq y_{\text{sup}}} B(\Delta y, \Delta\phi) dy}, \quad (4)$$

where  $y_{\text{inf/sup}}$  defines the lower/upper integration limit for different rapidity intervals depending on the kinematic region of interest.

## 3. HV phenomenology

In most HV models [16], the SM gauge group sector  $G_{\text{SM}}$  is extended by (at least) a new gauge group  $G_V$  under which all SM particles are neutral. Hence, a new category of  $v$ -particles emerges charged under  $G_V$ , but neutral under  $G_{\text{SM}}$ . Moreover, “communicators”, charged under both  $G_{\text{SM}}$  and  $G_V$ , are introduced to the theory allowing interactions between SM and HV particles. Communicators can be either intermediate (very massive) vector  $Z_v$  bosons, or hidden partners of the SM quarks and leptons, generically denoted as  $F_v$ , assumed to be pair-produced. In this study,  $F_v$  are taken as fermions (spin = 1/2) and  $q_v$  scalars.

Different mechanisms can connect the hidden and SM sectors through communicators, e.g., via the tree-level channel:  $e^+e^- \rightarrow Z_v \rightarrow q_v \bar{q}_v \rightarrow \text{hadrons}$ . Alternatively, communicators can be pair produced via SM  $\gamma^*/Z$  coupling to a  $F_v \bar{F}_v$  pair, yielding both visible and invisible cascades in the same event. We have checked that the latter channel significantly dominates over the former within the range of energies under study.

For some values of the HV parameter space, communicators can *promptly* decay into a particle  $f$  of the visible sector (its SM partner) and a  $q_v$  of the hidden sector according to the splitting:  $F_v \rightarrow f q_v$ .

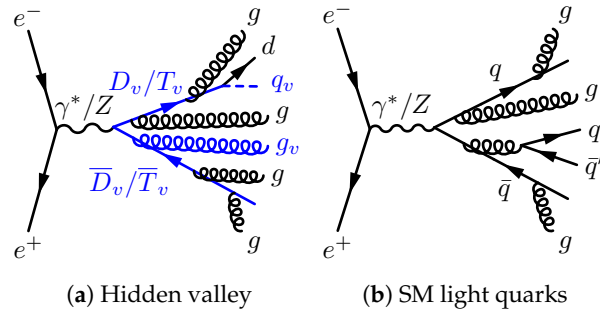


**Figure 1.** Leading diagrams of production in  $e^+e^-$  collisions for ((a)) HV, and ((b)) SM light quarks including bottom.

Note that the  $q_v$  mass may strongly influence the kinematics of the visible cascade (leading to SM particles) in the same event, thereby yielding observational consequences. This mass remains currently unconstrained ranging from zero to close to the  $F_v$  mass [17], so that different values of it will be assumed in our analysis.

Indeed, we are especially interested in the influence of the invisible (HV) sector on the partonic cascade into final-state SM particles, leading to potentially observable effects. This can be understood, e.g., as both visible and hidden cascades have to share the event's total energy, thereby modifying their respective available phase spaces. For the sake of concreteness, we restrict our study to a QCD-like HV scenario with  $q_v$ -quarks,  $g_v$ -gluons, and an equivalent “strong” coupling constant  $\alpha_v$ . For simplicity,  $\alpha_v$  is assumed not running with energy but fixed to  $\alpha_v = 0.1$ , as no significant differences were found in our analysis by varying this value.

#### 4. Analysis at detector level

To assess the feasibility of HV signal detection in  $e^+e^-$  colliders, we have relied throughout on the PYTHIA8 Monte Carlo event generator [18] because of its firmly established reliability and the fact that the HV production channel is already built in. Fast detector simulations were performed using the SGV tool [19] and the geometry and acceptances corresponding to the large model of the ILD concept for the International Linear Collider (ILC) as described in [20]. The simulated events are provided in the same event model as used by the ILD concept group, and the tools available in the ILCSoft package are used for the event reconstruction and analysis. The ILD reconstruction is based on the so-called Particle Flow approach, which aims to reconstruct all individual particles produced in the final state via pattern recognition algorithms. The reconstructed candidates of single particles are called Particle Flow Objects (PFOs). In our study, including detector effects, we set the centre-of-mass energy  $\sqrt{s}$  of  $e^+e^-$  collisions equal to 250 GeV to coincide with the planned first commissioning of the collider as a Higgs boson factory. As a further outlook, we extended our prospective study (this time only at particle level) up to  $\sqrt{s} = 500$  GeV and 1 TeV. The case of longitudinally polarised beams will be addressed in a future work once this option becomes available.

**Table 1.** Inclusive cross-sections for  $e^+e^- \rightarrow D_v\bar{D}_v$ ,  $e^+e^- \rightarrow q\bar{q}$  and  $WW \rightarrow 4q$  processes at  $\sqrt{s} = 250$  GeV, with different assignments for the  $m_{D_v}$  and  $m_{q_v}$  masses. Efficiencies of the selection criteria described in the main text, average charged-track multiplicities and their RMS, are shown.

Process	$m_{D_v}$ [GeV]	$m_{q_v}$ [GeV]	$\sigma_{\text{PYTHIA8}}$ [pb]	Efficiency [%]	$\langle N_{\text{ch}} \rangle$
$e^+e^- \rightarrow D_v\bar{D}_v$	125	0.1	0.13	36	$12.4 \pm 3.7$
	125	10	0.12	36	$12.4 \pm 3.7$
	125	50	0.12	42	$11.4 \pm 3.5$
	125	100	0.12	42	$6.5 \pm 2.1$
	100	50	1.29	42	$11.1 \pm 3.4$
	80	40	1.54	36	$18.0 \pm 4.9$
$e^+e^- \rightarrow q\bar{q}$ with ISR			48	$\lesssim 0.01$	$9.9 \pm 3.4$
$WW \rightarrow 4q$			7.4	$\lesssim 0.001$	–

As already commented in the previous section, the HV signal proceeds via the process  $e^+e^- \rightarrow D_v\bar{D}_v \rightarrow$  hadrons (where  $D_v$  denotes the lightest communicator, being the hidden partner of the  $d$ -quark) as depicted in Fig. 1(a). In our benchmark scenarios we set  $\alpha_v = 0.1$ ,  $m_{D_v} = 125$  GeV, with four different  $v$ -quark mass values:  $m_{q_v} = 0.1, 10, 50$  and  $100$  GeV. We also consider  $m_{D_v} = 80$  and  $100$  GeV with  $m_{q_v} = 40$  and  $50$  GeV respectively. At higher  $\sqrt{s}$ , we also included  $T_v\bar{T}_v$  pair production, assuming that it becomes kinematically possible.

In our analysis at  $\sqrt{s} = 250$  GeV, the  $e^+e^- \rightarrow q\bar{q}$  background comes from the inclusive production of all the SM quark species except the top flavour, since its production lies below threshold (see Fig. 1).

In a preceding investigation [21], the aforementioned signal and background were examined at particle level. Besides, no Initial State Radiation (ISR) was included although it plays a crucial role in the analysis, as we shall see soon. Four-fermion production (dominated by  $e^+e^- \rightarrow WW$ ) was neither considered but its contribution has been found to be negligible. In the present work, we broaden our study to detector level, taking into account the ISR effect, which enables the production of the large cross-section process  $e^+e^- \rightarrow \gamma Z$  with the  $Z$  being produced on-shell and decaying afterwards. The cross-sections for the HV and SM processes have been estimated from PYTHIA8 reported in Table 1.

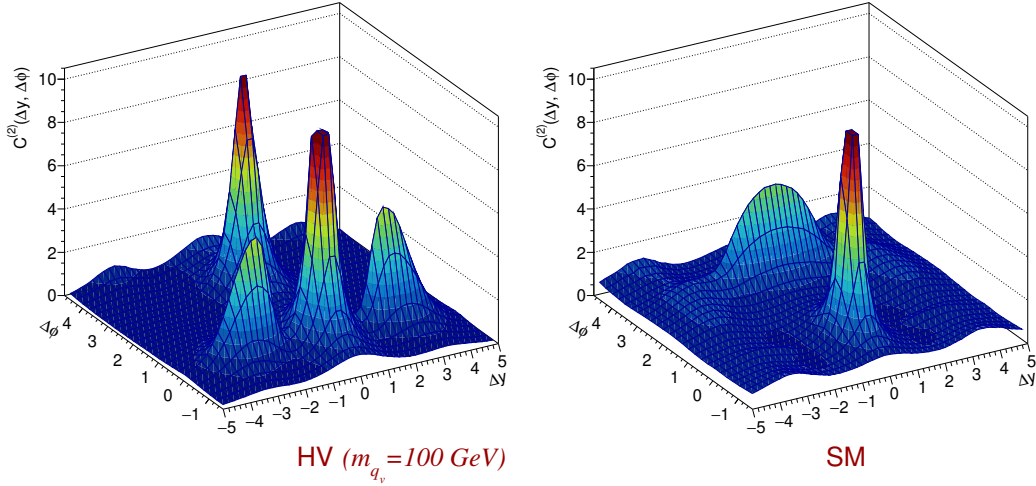
In view of the small cross-sections for HV production from Table 1, specific cuts have to be implemented to maximise the background removal while keeping the signal as much as possible. On the other hand, displaced vertices due to the production and decay of long-lived particles have not been considered here as we are focusing on prompt decays of  $v$ -particles and their effect on the partonic cascade yielding final-state SM particles. Following a similar strategy as in [22], a set of selection cuts have been defined. The final selection-cut efficiency, reported in Table 1, shows a drastic reduction of the SM background while the HV signal is affected to a much lesser extent.

**Table 2.** Breakdown of accumulated efficiencies of the selection criteria described in the main text. For simplicity, only one HV model is shown, since results are very similar for the rest:  $e^+e^- \rightarrow D_v\bar{D}_v$  with  $m_{D_v} = 125$  GeV and  $m_{q_v} = 100$  GeV. The two SM processes described in the text and in Table 1 are also shown. The definition of the cuts, S1 – S3 and B1 are defined in the text. In this table we also differentiate between the  $q\bar{q}$ -RR (dominated by radiative return events) and the  $q\bar{q}$ -Cont. in the continuum (*i.e.*, with  $m_{q\bar{q}}^{inv} \sim \sqrt{s}$  at partonic level and before parton shower).

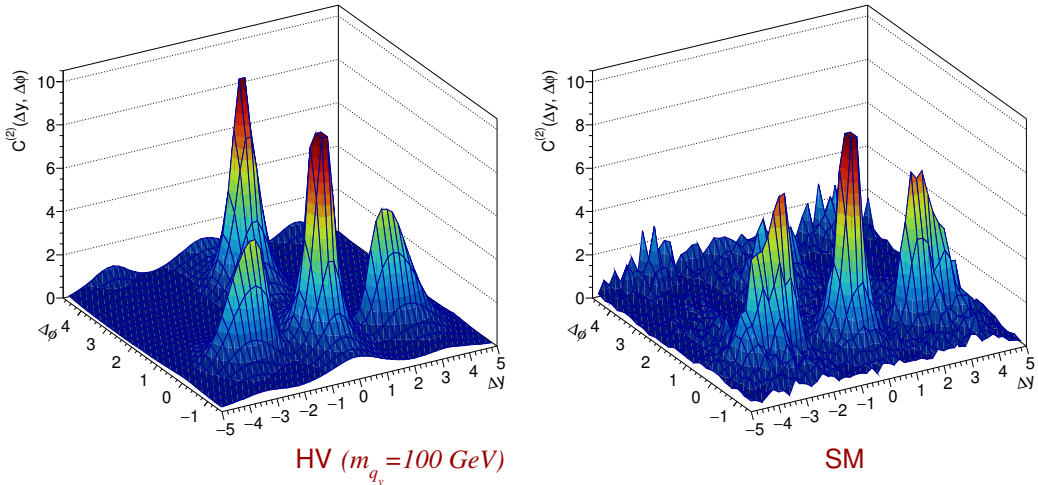
Cuts	HV	Efficiency [%]		
		$q\bar{q}$ -RR	$4q$	$q\bar{q}$ -Cont.
S1 = Multiplicity	89	30	64	40
S1+S2 = S1+ISR photon	42	3.8	12	8.8
S1+S2+S3 = S1+S2+Energy and invariant. mass	42	$\lesssim 0.01$	$\lesssim 0.001$	–
S1+S2+B1 = S1+S2+Thrust	–	–	–	5.6

The selection cuts applied in this analysis are the following. S1: constraints have been set on the number of displaced vertices per jet (= 0) and the number of neutral and charged PFOs ( $\leq 22$  and  $\leq 15$ ,

respectively); S2: cuts are applied on the reconstructed ISR photon candidates angle ( $|\cos \theta_{\gamma_{\text{ISR}}}| < 0.5$ ) and energy ( $E_{\gamma_{\text{ISR}}} < 40$  GeV); S3: constraints on the di-jet invariant mass ( $m_{jj} < 130$  GeV) and on the energy of the most energetic jet ( $E < 80$  GeV); B1, a thrust value larger than ( $T > 0.95$ ) was imposed. The S1 – S3 cuts are applied to the evaluation of  $S(\Delta y, \Delta\phi)$ , while for the evaluation of  $B(\Delta y, \Delta\phi)$ , S1 – 2 and B1 are applied. The selection efficiencies for different combinations of these cuts applied to different processes are displayed in Table 2.



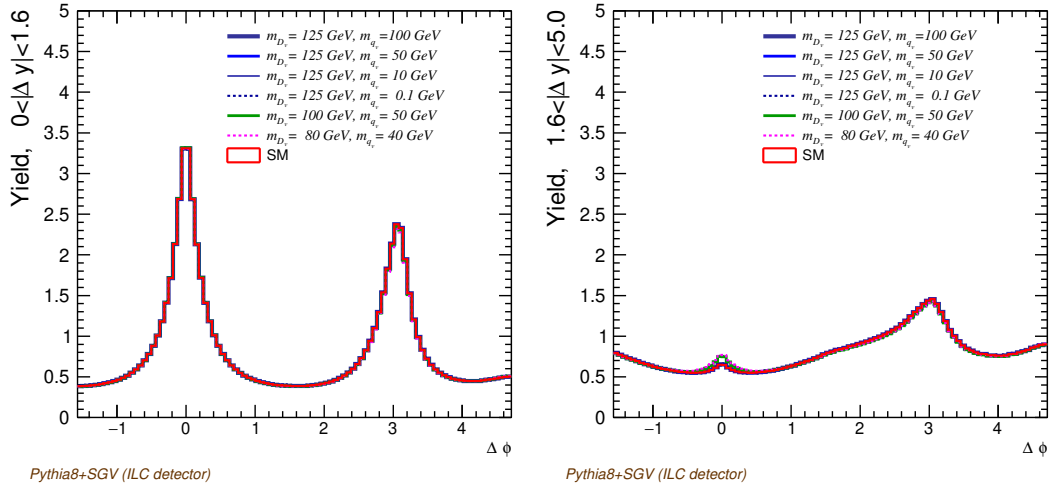
(a) Detector level distributions with no selection applied to the  $S(\Delta y, \Delta\phi)$  reconstruction.



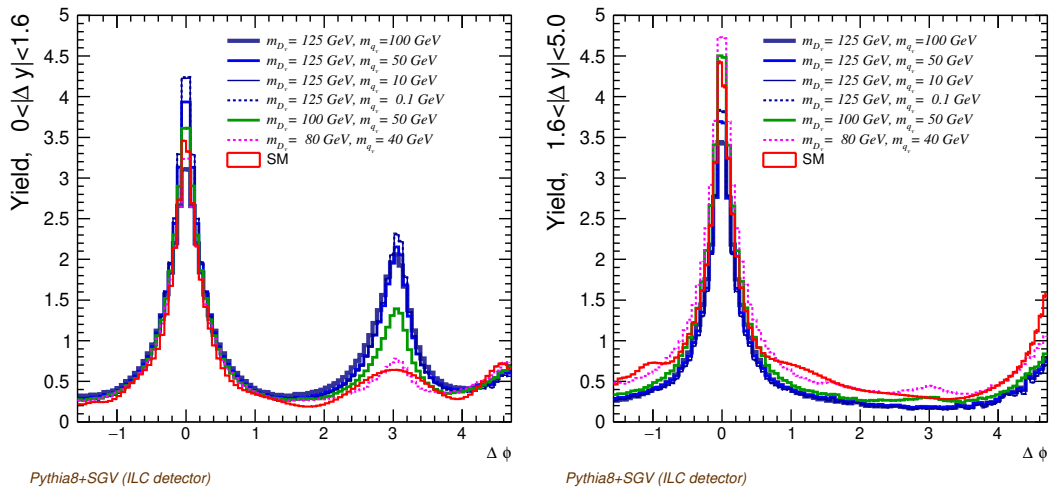
(b) Detector level distributions after the signal enriching experimental cuts applied to the  $S(\Delta y, \Delta\phi)$  reconstruction.

**Figure 2.** 3D plots of the two-particle angular correlation function,  $C^{(2)}(\Delta y, \Delta\phi)$ , at detector level, separately for the pure HV signal and the SM background in  $e^+e^-$  collisions at  $\sqrt{s} = 250$  GeV. In the pure HV case,  $m_{q_v} = 100$  GeV,  $m_{D_v} = 125$  GeV and  $\alpha_v = 0.1$  were set. For the SM case, light quarks include the bottom flavour.

Figure 2 shows three-dimensional plots of the two-particle correlation function  $C^{(2)}(\Delta y, \Delta\phi)$  separately for the HV and SM scenarios, before (Fig. 2(a)) and after (Fig. 2(b)) cuts. As a reference example, in the HV case we set  $m_{q_v} = 100$  GeV,  $m_{D_v} = 125$  GeV and  $\alpha_v = 0.1$  alongside the decay  $D_v \rightarrow d + q_v$  initiating the partonic (both visible and invisible) shower. As expected, a near-side peak shows up at  $(\Delta y \simeq 0, \Delta\phi \simeq 0)$ , receiving contributions mainly from track pairs within the same jet. On the other hand, an away-side correlation ridge around  $\Delta\phi \simeq \pi$ , and extending over a large rapidity range, results from back-to-back momentum balance, in principle unrelated to NP effects. After cuts, a near-side ridge (with two pronounced and symmetric bumps) shows up for  $1.6 < |\Delta y| < 3$  at  $\Delta\phi \simeq 0$



(a) Detector-level yield distributions with no selection cuts applied.

(b) Detector-level yield distributions after the selection cuts were applied to enrich the  $S(\Delta y, \Delta\phi)$  sample with HV signal events.

**Figure 3.** Yield  $Y(\Delta\phi)$  for both HV signal in association with SM and for pure SM background (red line) for the  $0 < |\Delta y| < 1.6$  (left) and  $1.6 < |\Delta y| < 5$  intervals (right), respectively. The  $S(\Delta y, \Delta\phi)$  used for the Yield calculation are defined as:

$$S^{SM}(\Delta y, \Delta\phi) = \frac{1}{N_{\text{pairs}}^{SM}} \frac{d^2 N_{\text{same}}^{SM}}{d\Delta y d\Delta\phi};$$

$$S^{SM+HV}(\Delta y, \Delta\phi) = \frac{1}{N_{\text{pairs}}^{SM} + N_{\text{pairs}}^{HV}} \left( \frac{d^2 N_{\text{same}}^{SM}}{d\Delta y d\Delta\phi} + \frac{d^2 N_{\text{same}}^{HV}}{d\Delta y d\Delta\phi} \right);$$

for the SM case, similar to the pure HV scenario. This structure arises from the ISR effect, since the effective center-of-mass energy approaches the Z mass, and thus resonant production greatly enhances the production cross-section. It becomes of paramount importance to take this effect into account in our analysis, mimicking possible HV signatures in angular correlations.

In order to examine in more detail the possibility of discriminating the HV signal from the pure SM background, we depict in Fig. 3 the yield  $Y(\Delta\phi)$  (defined in Eq. (4)) for both  $0 < |\Delta y| \leq 1.6$  and  $1.6 < |\Delta y| < 5$  ranges: before (Fig. 3(a)) and after (Fig. 3(b)) cuts. Note that the HV signal for various masses  $m_{D\nu}, m_{q\nu}$  is considered together with the SM background, while a standalone analysis of the SM background is also presented. A clear difference becomes apparent for  $0 < |\Delta y| \leq 1.6$ : a sizeable peak at  $\Delta\phi \sim \pi$  characterises the HV scenario, unlike the pure SM case. This remarkable discrepancy

**Table 3.** Inclusive cross-sections of the HV signal and SM background at  $\sqrt{s} = 500$  GeV and  $\sqrt{s} = 1$  TeV. Cross-section predictions do not depend on the  $m_{q_v}$  value unless it is too large to make the process kinematically inaccessible. The signal corresponds to  $D_v$  and  $T_v$  pair production with the  $D_v/T_v$  mass set equal to  $\sqrt{s}/2$ . Whenever kinematically allowed,  $t\bar{t}$  production has been included as a SM background source in addition to lighter flavours considered at  $\sqrt{s} = 250$  GeV.

Process	$\sigma_{\sqrt{s}=500\text{GeV}}$ [pb]	$\sigma_{\sqrt{s}=1\text{TeV}}$ [pb]
$e^+e^- \rightarrow D_v\bar{D}_v$	$2.4 \times 10^{-2}$ ( $m_{D_v} = 250$ GeV)	$4.4 \times 10^{-3}$ ( $m_{D_v} = 500$ GeV)
$e^+e^- \rightarrow T_v\bar{T}_v$	$9.5 \times 10^{-2}$ ( $m_{T_v} = 250$ GeV)	$1.8 \times 10^{-2}$ ( $m_{T_v} = 500$ GeV)
$e^+e^- \rightarrow q\bar{q}$ with ISR	11	2.9
$e^+e^- \rightarrow t\bar{t}$	0.59	0.19
$WW \rightarrow 4q$	3.4	1.3

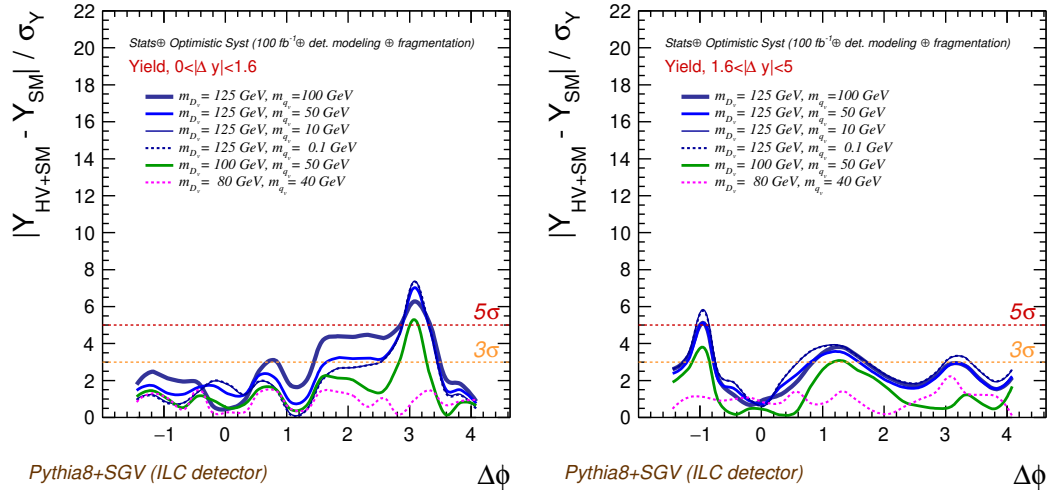
of shapes would potentially serve as a valuable signature of a hidden sector, complementary to more conventional BSM searches, as claimed in this study.

## 5. Prospects on the experimental sensitivity

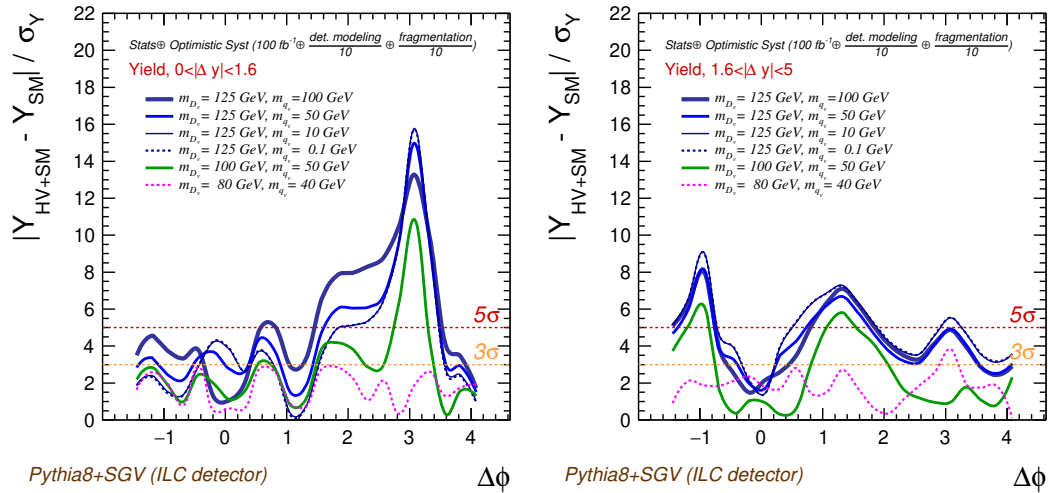
Let us stress that an analysis to search for BSM physics in high-energy collisions relying on angular correlations (as proposed in this paper) offers several advantages with respect to more conventional methods, e.g., based on an excess of events in cross sections or invariant mass peaks. In particular, yield distributions as defined in Eq.(4) benefit from an almost total cancellation of reconstruction efficiencies and detector acceptances, luminosity and cross-section dependence, etc. However, modelling uncertainties could be a limiting factor for these observables. In order to better understand this issue, we performed a study assuming different scenarios for the foreseen statistic and systematic uncertainties.

To estimate the statistical uncertainties, we assume a collected luminosity of  $100 \text{ fb}^{-1}$ , which roughly corresponds to one year of data taking of ILC in the H20-staged scenario [23]. For the systematic uncertainties, we identified two potential main sources: the detector performance modelling and the fragmentation (pertaining to the final hadronisation of the partonic cascade) uncertainties. For both of them, only educated guesses based on current knowledge can be made. For instance, the detector performance modelling uncertainty is evaluated by a bin-by-bin comparison of the estimated yield distributions at particle and detector levels. The absolute value of the difference is taken as uncertainty. This comparison should account for the kinematic resolution (including angular) on the track reconstruction, as well as acceptance effects. We stress that this approach highly overestimates the experimental uncertainties, therefore, it represents a worst-case scenario. For the fragmentation uncertainty, we follow the same recipe as for the detector-effects modelling, but this time we compare the predictions of the yield at the particle level calculated using two different fragmentation models implemented in PYTHIA8 and HERWIG 7.3 [24,25], respectively. The total uncertainty, calculated also bin by bin, is composed of the addition in quadrature of the statistical uncertainty for the expected number of events, and the systematic uncertainties of  $Y_{SM}$  since only PYTHIA8 includes Hidden Valley production. The outcome of these assumptions is summarised in Fig. 4, with  $\sigma_Y$  representing the estimated uncertainty as explained above.

Once all the above points are taken into account, it is straightforward to calculate the sensitivity of the observable by comparing the HV and SM predictions for  $Y$  with the expected uncertainties. Already at  $100 \text{ fb}^{-1}$ , the sensitivity is mostly limited by systematic uncertainties as the detector performance systematics is dominant over all the others. However, the discovery power remains almost intact, especially near the sizeable  $Y$  peak at  $\Delta\phi \sim \pi$  with  $0 < |\Delta y| \leq 1.6$ . As an exercise, we compare the estimated sensitivity with a much more optimistic scenario in which we improve our knowledge of systematic uncertainties by one order of magnitude with respect to the current estimates assuming a significant improvement in detector-performance-related uncertainties. Dedicated studies on the fragmentation modelling of HV processes would also be required for further understanding. Assuming



(a) With systematic modelling uncertainties obtained from current state of the art.



(b) Same as above but assuming an improvement of one order magnitude on the modelling uncertainties evaluation.

**Figure 4.** Expected experimental sensitivity for Hidden Valley models along with the SM background after collecting  $100 \text{ fb}^{-1}$  of integrated luminosity, for yield measurements in the range of  $0 < |\Delta y| < 1.6$  (left) and  $1.6 < |\Delta y| < 5$ . (right). The experimental sensitivity is expected to be dominated by systematic uncertainties associated with the detector response and parton shower and fragmentation modelling.

this order of magnitude improvement, the sensitivity would be drastically enhanced, and the discovery power would be reached for most of the phase space available. Of course, we emphasise that this is only an educated guess that should serve as yet another motivation to pursue the best possible design of future collider detectors and progress on Monte Carlo tools development to minimise modelling uncertainties.

## 6. Different energies and colliders

Till now, we have focused on a future  $e^+e^-$  collider operating at  $\sqrt{s} = 250 \text{ GeV}$ , but likely those machines will later run at higher energies. Therefore we have extended our study to  $\sqrt{s} = 0.5$  and  $1 \text{ TeV}$ , at particle level for the time being.

As the HV signal  $e^+e^- \rightarrow Q_v \bar{Q}_v \rightarrow \text{hadrons}$ , we consider the two extreme cases: the lightest communicator  $D_v$  and the heaviest one  $T_v$  which decays into  $q_v t$ . We have confirmed that intermediate masses yield intermediate results. Besides the  $q\bar{q}$  and  $WW \rightarrow 4q$  backgrounds, we also take into

account the production of  $t\bar{t}$ , which, in fact, becomes relevant at these energies. Table 3 presents the cross-sections obtained from PYTHIA8. We set the mass of  $D_v$  and  $T_v$  equal to  $\sqrt{s}/2$ , and results for different  $m_{q_v}$  are shown. No large variations are obtained around this mass assignment to the communicator. According to expectations, the contribution from the SM backgrounds decreases with energy. For the HV signal, a reduction of the cross-section by two orders of magnitude is obtained at  $\sqrt{s} = 1$  TeV.

This study is also relevant for the  $e^+e^-$  option of the Future Circular Collider (FCC) operating at an energy of  $\sqrt{s} = 240$  GeV, i.e. very near to the one assumed so far. The limited coverage in the forward region makes the ISR-photon detection less efficient, yet the pertinent optimisation of selection cuts recovers sensitivity to a HV signal [26].

## 7. Conclusions

The analysis of particle correlations in high-energy colliders can provide valuable insights into matter under extreme temperature and density conditions, somehow reproducing the early-universe conditions when quarks and gluons had not yet bound to form hadrons. On the other hand, this kind of analysis can become a complementary tool to other conventional searches to uncover the existence of new phenomena including BSM physics as postulated in Refs. [27,28] and studied in this work.

Motivated by the experimental observation of unexpected structures shown in angular correlations from hadronic collisions, we have explored at detector level the discovery potential for hidden sectors at future  $e^+e^-$  colliders using two-particle angular correlations. Specifically, we consider a QCD-like HV model containing not-too-heavy  $v$ -quarks and  $v$ -gluons, which can interact with the SM sector via communicators of mass, typically  $\lesssim 1$  TeV. We have focused on  $D_v\bar{D}_v$  pair production at  $\sqrt{s} = 250$  GeV, of the order of the expected mass for the lightest communicator in this scenario. We have briefly extended our study at the particle level to higher energies (up to 1 TeV), pointing out promising prospects too.

To conclude, our results show that two-particle azimuthal correlations in a  $e^+e^-$  Higgs factory could indeed become a useful tool for discovering NP if it is kinematically accessible. Although a specific HV model has been employed, other types of hidden sectors would expectedly yield similar signatures. In addition, collective effects stemming from a source different from BSM cannot be excluded in this kind of analysis. Such searches, based on rather diffuse signals that spread over a large number of final-state particles, should be contemplated as complementary to other more conventional methods, thereby increasing the discovery potential of these machines.

**Acknowledgments:** We thank M. Berggren and the ILD software working group for their support with the usage of detector fast simulation and the reconstruction tools employed in this study. AI, EM and VAM acknowledge support by Spanish MCIU/ AEI / 10.13039/501100011033 and European Union / FEDER via the grant PID2021-122134NB-C21. EM and VAM acknowledge support by Generalitat Valenciana (GV) via the Excellence Grant CIPROM/2021/073. AI acknowledges support by GV under the grant number CIDEAGENT/2020/21, the financial support from the MCIN with funding from the European Union NextGenerationEU and by GV via the Programa de Planes Complementarios de I+D+i (PRTR 2022) Project *Si4HiggsFactories*, reference ASFAE/2022/015. IC acknowledges support by the Xunta de Galicia (CIGUS Network of Research Centers). MASL acknowledges support from the Spanish Agency Estatal de Investigacion under Grant PID2023-151418NB-I00 funded by MCIU/AEI/10.13039/501100011033/ FEDER, UE and by GV under grant CIPROM/2022/36. AI, EM, VAM and MASL acknowledge support by the Spanish MCIU/AEI via the Severo Ochoa project CEX2023-001292-S.

1. Kittel, W.; De Wolf, E.A. *Soft multihadron dynamics*; World Scientific, 2005. <https://doi.org/10.1142/5805>.
2. Botet, R.; Ploszajczak, M. *Universal fluctuations: The phenomenology of hadronic matter*; World Scientific, 2002. <https://doi.org/10.1142/4916>.
3. Khachatryan, V.; et al. Measurement of long-range near-side two-particle angular correlations in pp collisions at  $\sqrt{s} = 13$  TeV. *Phys. Rev. Lett.* **2016**, *116*, 172302, [arXiv:nucl-ex/1510.03068]. <https://doi.org/10.1103/PhysRevLett.116.172302>.

4. Abelev, B.; et al. Long-range angular correlations on the near and away side in  $p$ -Pb collisions at  $\sqrt{s_{NN}} = 5.02$  TeV. *Phys. Lett. B* **2013**, *719*, 29–41, [arXiv:nucl-ex/1212.2001]. <https://doi.org/10.1016/j.physletb.2013.01.012>.
5. Aad, G.; et al. Observation of Associated Near-Side and Away-Side Long-Range Correlations in  $\sqrt{s_{NN}} = 5.02$  TeV Proton-Lead Collisions with the ATLAS Detector. *Phys. Rev. Lett.* **2013**, *110*, 182302, [arXiv:hep-ex/1212.5198]. <https://doi.org/10.1103/PhysRevLett.110.182302>.
6. Shuryak, E.V. On the origin of the ‘Ridge’ phenomenon induced by jets in heavy ion collisions. *Phys. Rev. C* **2007**, *76*, 047901, [arXiv:nucl-th/0706.3531]. <https://doi.org/10.1103/PhysRevC.76.047901>.
7. Dumitru, A.; Gelis, F.; McLerran, L.; Venugopalan, R. Glasma flux tubes and the near side ridge phenomenon at RHIC. *Nucl. Phys. A* **2008**, *810*, 91–108, [arXiv:hep-ph/0804.3858]. <https://doi.org/10.1016/j.nuclphysa.2008.06.012>.
8. Bozek, P.; Broniowski, W. Collective dynamics in high-energy proton-nucleus collisions. *Phys. Rev. C* **2013**, *88*, 014903, [arXiv:nucl-th/1304.3044]. <https://doi.org/10.1103/PhysRevC.88.014903>.
9. Sanchis-Lozano, M.A.; Sarkisyan-Grinbaum, E. A correlated-cluster model and the ridge phenomenon in hadron–hadron collisions. *Phys. Lett. B* **2017**, *766*, 170–176, [arXiv:hep-ph/1610.06408]. <https://doi.org/10.1016/j.physletb.2017.01.001>.
10. Sanchis-Lozano, M.A.; Sarkisyan-Grinbaum, E. Ridge effect and three-particle correlations. *Phys. Rev. D* **2017**, *96*, 074012, [arXiv:hep-ph/1706.05231]. <https://doi.org/10.1103/PhysRevD.96.074012>.
11. Noronha, J.; Schenke, B.; Shen, C.; Zhao, W. Progress and Challenges in Small Systems. 1 2024, [arXiv:nucl-th/2401.09208].
12. Badea, A.; Baty, A.; Chang, P.; Innocenti, G.M.; Maggi, M.; McGinn, C.; Peters, M.; Sheng, T.A.; Thaler, J.; Lee, Y.J. Measurements of two-particle correlations in  $e^+e^-$  collisions at 91 GeV with ALEPH archived data. *Phys. Rev. Lett.* **2019**, *123*, 212002, [arXiv:hep-ex/1906.00489]. <https://doi.org/10.1103/PhysRevLett.123.212002>.
13. Chen, Y.C.; et al. Measurement of Two-Particle Correlations of Hadrons in  $e^+e^-$  Collisions at Belle. *Phys. Rev. Lett.* **2022**, *128*, 142005, [arXiv:hep-ex/2201.01694]. <https://doi.org/10.1103/PhysRevLett.128.142005>.
14. Chen, Y.C.; et al. Long-range near-side correlation in  $e^+e^-$  collisions at 183–209 GeV with ALEPH archived data. *Phys. Lett. B* **2024**, *856*, 138957, [arXiv:hep-ex/2312.05084]. <https://doi.org/10.1016/j.physletb.2024.138957>.
15. Gelis, F.; Iancu, E.; Jalilian-Marian, J.; Venugopalan, R. The Color Glass Condensate. *Ann. Rev. Nucl. Part. Sci.* **2010**, *60*, 463–489, [arXiv:hep-ph/1002.0333]. <https://doi.org/10.1146/annurev.nucl.010909.083629>.
16. Strassler, M.J.; Zurek, K.M. Echoes of a hidden valley at hadron colliders. *Phys. Lett. B* **2007**, *651*, 374–379, [hep-ph/0604261]. <https://doi.org/10.1016/j.physletb.2007.06.055>.
17. Pérez-Ramos, R.; Sanchis-Lozano, M.A.; Sarkisyan-Grinbaum, E.K. Searching for hidden matter with long-range angular correlations at  $e^+e^-$  colliders. *Phys. Rev. D* **2022**, *105*, 053001, [arXiv:hep-ph/2110.05900]. <https://doi.org/10.1103/PhysRevD.105.053001>.
18. Sjöstrand, T.; Ask, S.; Christiansen, J.R.; Corke, R.; Desai, N.; Ilten, P.; Mrenna, S.; Prestel, S.; Rasmussen, C.O.; Skands, P.Z. An introduction to PYTHIA 8.2. *Comput. Phys. Commun.* **2015**, *191*, 159–177, [arXiv:hep-ph/1410.3012]. <https://doi.org/10.1016/j.cpc.2015.01.024>.
19. Berggren, M. SGV 3.0 – a fast detector simulation **2012**. [arXiv:physics.ins-det/1203.0217].
20. Abramowicz, H.; et al. International Large Detector: Interim Design Report **2020**. [arXiv:physics.ins-det/2003.01116].
21. Musumeci, E.; Perez-Ramos, R.; Irls, A.; Corredoira, I.; Mitsou, V.A.; Sarkisyan-Grinbaum, E.; Sanchis-Lozano, M.A. Two-particle angular correlations in the search for new physics at future  $e^+e^-$  colliders. In Proceedings of the International Workshop on Future Linear Colliders, 7 2023, [arXiv:hep-ph/2307.14734].
22. Irls, A.; Márquez, J.P.; Pöschl, R.; Richard, F.; Saibel, A.; Yamamoto, H.; Yamatsu, N. Probing gauge-Higgs unification models at the ILC with quark–antiquark forward–backward asymmetry at center-of-mass energies above the Z mass. *Eur. Phys. J. C* **2024**, *84*, 537, [arXiv:hep-ph/2403.09144]. <https://doi.org/10.1140/epjc/s10052-024-12918-z>.
23. Bambade, P.; et al. The International Linear Collider: A Global Project **2019**. [arXiv:hep-ex/1903.01629].
24. Bahr, M.; et al. Herwig++ Physics and Manual. *Eur. Phys. J. C* **2008**, *58*, 639–707, [arXiv:hep-ph/0803.0883]. <https://doi.org/10.1140/epjc/s10052-008-0798-9>.
25. Bellm, J.; et al. Herwig 7.0/Herwig++ 3.0 release note. *Eur. Phys. J. C* **2016**, *76*, 196, [arXiv:hep-ph/1512.01178]. <https://doi.org/10.1140/epjc/s10052-016-4018-8>.

26. Musumeci, E.; Irlles, A.; Perez-Ramos, R.; Corredoira, I.; Sarkisyan-Grinbaum, E.; Mitsou, V.A.; Sanchis-Lozano, M.A. Hidden sectors at FCC-ee with two-particle angular correlations, 2024. <https://doi.org/10.17181/nyvbx-aw669>.
27. Sanchis-Lozano, M.A. Prospects of searching for (un)particles from Hidden Sectors using rapidity correlations in multiparticle production at the LHC. *Int. J. Mod. Phys. A* **2009**, *24*, 4529–4572, [arXiv:hep-ph/0812.2397]. <https://doi.org/10.1142/S0217751X09045820>.
28. Sanchis-Lozano, M.A.; Sarkisyan-Grinbaum, E.K. Searching for new physics with three-particle correlations in  $pp$  collisions at the LHC. *Phys. Lett. B* **2018**, *781*, 505–509, [arXiv:hep-ph/1802.06703]. <https://doi.org/10.1016/j.physletb.2018.04.033>.